PERGAMON

International Journal of Solids and Structures 38 (2001) 3393–3409

INTERNATIONAL JOURNAL OF SOLIDS and STRUCTURES

www.elsevier.com/locate/ijsolstr

A two-dimensional shape memory alloy/elastomer actuator

Faramarz Gordaninejad *, Weida Wu

Department of Mechanical Engineering, University of Nevada, Mail Stop 312, Reno, NV 89557-0154, USA

Received 29 November 1999; in revised form 27 March 2000

Abstract

This paper presents a theoretical model for the response of a two-dimensional, thermally driven, shape memory alloy (SMA)/elastomer actuator. The actuator is assumed to be constructed from a thin layer of SMA bonded to a layer of elastomer. The proposed device is considered to undergo small displacements and small strains. The governing equations are developed utilizing the classical laminated plate theory, energy balance equations, and a two-dimensional transition model of the SMA layer. A finite element model is developed to solve the nonlinear system of equations. Parametric studies are conducted to demonstrate the effects of the elastomer thickness, thermal conductivity, input energy, and heat sink strength on the overall time response of the SMA/elastomer actuator.

Keywords: Shape memory alloy; Elastomer; Actuator; Two-dimensional; Time response; Thermal conductivity; Heat sink strength; Input power

1. Introduction

The focus of this study is on the responses of a proposed shape memory alloy (SMA)/elastomer actuator. The actuator is assumed to be constructed from a thin layer of SMA bonded to a matrix of elastomer. The present work is the extension of the study by Wu et al. (1996), in which the temperature–stress–strain and time responses of a SMA/elastomer beam were investigated by using a shear-lag stress model.

The SMA as an actuator has been widely studied in recent years. For example, Rogers and Baker (1990) demonstrated an application of SMA composite for active structural vibration control of a clamped–clamped graphite/epoxy beam with embedded SMA actuators at the neutral axis. The application of the SMA reinforced composite in structural acoustic radiation control was investigated by Saunders et al. (1991). Baz and Tampe (1989) have shown that discrete SMA actuators can be used to control buckling of flexible structures. Lagoudas and Tadjbakhsh (1993) studied a generalized theory to model the resultant forces and moments for a flexible rod with an embedded line actuator.

Models to simulate the martensitic transformation were developed by Tanaka (1982), and Liang and Rogers (1990). Also, a one-dimensional thermo-mechanical constitutive relation for SMAs was developed

* Corresponding author. Tel.: +1-775-784-6990; fax: +1-775-784-1701.
E-mail address: faramarz@unr.edu (F. Gordaninejad).

0020-7683/01/$ - see front matter
PII: S0020-7683(00)00265-1

Nomenclature

A	actuator length
A_s	austenite start temperature
A_f	austenite finish temperature
B	actuator width
c	specific heat
C	thermal capacity
E_n	Young's modulus of the SMA
E_e	Young's modulus of the elastomer
h	actuator thickness
k_n	thermal conductivity of the SMA
k_e	thermal conductivity of the elastomer
M_s	martensite start temperature
M_f	martensite finish temperature
P	input power
q	transverse load
q_x	heat flux in x direction
q_y	heat flux in y direction
Q_n	heat of transition (latent heat)
Q_x	shear stress resultant on xz plane
Q_y	shear stress resultant on yz plane
R_k	dimensionless thermal conductivity
R_{MA}	dimensionless heat of transition
R_P	dimensionless input power
S	heat sink strength
t	time
t_n	SMA layer thickness
T	temperature
T_0	heat sink temperature
u	in-plane axial displacement
v	in-plane transverse displacement
w	out-of-plane deflection
W	dimensionless out-of-plane deflection
x	coordinate
y	coordinate
X	dimensionless coordinate
Y	dimensionless coordinate
Φ	dimensionless transverse load
θ_x	rotation in xz plane
θ_y	rotation in yz plane
Θ	dimensionless temperature
ρ	density
σ_x	normal stress in x direction
σ_y	normal stress in y direction
τ	dimensionless time
τ_{xy}	shear stress in xy plane
ξ	martensite fraction

by Rogers et al. (1989). In order to simulate the thermal-stress behavior of a SMA in a two-dimensional geometry, Ikuta and Shimizu (1993) introduced the so-called "variable sublayer model."

In this study, a two-dimensional nonlinear transient analysis of a thermally driven SMA/elastomer actuator is presented. The classical laminated plate theory is utilized. The energy balance equation is developed to model the thermal behavior of the SMA layer. The nonlinear constitutive equations for the SMA layer is obtained by combining the actuator's constitutive equations with the variable sublayer model for the two-dimensional martensitic transformation. The governing system of equations is solved by using a finite element method.

2. Shape memory alloy/elastomer actuator modeling

Let us consider the SMA/elastomer actuator shown in Fig. 1a and b, in which the xy plane coincides with the midplane. The actuator is composed of two isotropic layers, a SMA layer with thickness, t_n, and an elastomer layer with thickness, $(h - t_n)$. The elastomer layer is bonded to a heat sink maintained at temperature T_0. It is assumed that the two layers are continuously bonded together. Simply supported boundary conditions at all four edges of the actuator are considered. The actuator is subjected to a uniformly distributed load, q.

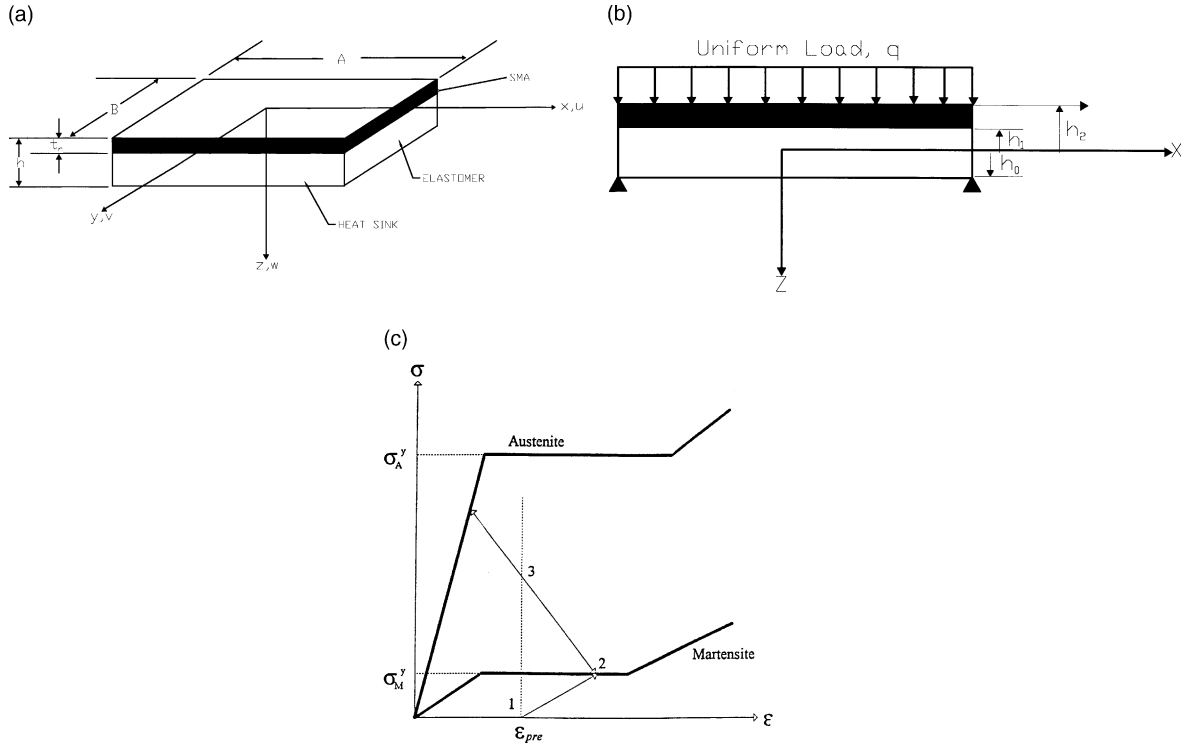

Fig. 1. (a) The geometry configuration of the proposed actuator. (b) The SMA/elastomer under external uniform load and simply supported boundary conditions at all four edges. (c) Modeling of the SMA layer stress–strain relation in austenite and martensite phases.

Initially, the SMA layer is pre-strained in the martensitic phase before the transverse load is applied. The stress–strain state in the SMA is indicated schematically as "state 1" in Fig. 1c. Due to the applied load, an additional elastic strain is built in the SMA layer, which is indicated as "state 2". When heated, by an electric current, above the austenite start temperature, A_s, the SMA transforms into the austenitic phase, attempting to recover both the elastic strain and the elastic pre-strain. Since the focus of this work is on the transient time response of the SMA layer, small deformation is considered. Hence, the recovered strain is kept within the linear elastic strain range (i.e., "state 3" indicated in Fig. 1c). This is the limit for the recovery strain. As a result of strain recovery process, the deflection of the actuator is reduced. After the electric current is reduced or removed, the SMA layer cools down (via conduction through the elastomer to the heat sink) to the martensite phase. When the SMA reaches the martensite phase, the stress–strain state of the SMA returns to "state 2."

The equilibrium equations for a general state of stress in the absence of body force are

$$\frac{\partial \sigma_x}{\partial x} + \frac{\partial \tau_{xy}}{\partial y} + \frac{\partial \tau_{xz}}{\partial z} = 0, \tag{1a}$$

$$\frac{\partial \sigma_y}{\partial y} + \frac{\partial \tau_{yx}}{\partial x} + \frac{\partial \tau_{yz}}{\partial z} = 0, \tag{1b}$$

$$\frac{\partial \sigma_z}{\partial z} + \frac{\partial \tau_{zx}}{\partial x} + \frac{\partial \tau_{zy}}{\partial y} = 0. \tag{1c}$$

Based on the microscopic observation of SMA behavior, in which the martensite and austenite phases are blended uniformly in the bulk metal during the martensite phase transformation, Ikuta and Shimizu (1993) proposed the so-called "variable sublayer model" to formulate the two-dimensional in-plane stresses in the SMA layer during the phase transformation, as follows:

$$\sigma_x(\xi) = (1-\xi)\sigma_{x\mathrm{A}} + \xi\sigma_{x\mathrm{M}}, \tag{2a}$$

$$\sigma_y(\xi) = (1-\xi)\sigma_{y\mathrm{A}} + \xi\sigma_{y\mathrm{M}}, \tag{2b}$$

$$\tau_{xy}(\xi) = (1-\xi)\tau_{xy\mathrm{A}} + \xi\tau_{xy\mathrm{M}}, \tag{2c}$$

where ξ is the martensite fraction, $\sigma_{x\mathrm{A}}$, $\sigma_{y\mathrm{A}}$ and $\tau_{xy\mathrm{A}}$ are the in-plane stresses of the SMA layer in the austenite phase, and $\sigma_{x\mathrm{M}}$, $\sigma_{y\mathrm{M}}$ and $\tau_{xy\mathrm{M}}$ are the in-plane stresses of the SMA layer in the martensite phase. In this study, it is assumed that the actuator can be modeled as a thin plate with the midplane of the plate remaining unstrained under bending; therefore, from the classical plate theory

$$u(x,y,z) = -z\theta_x(x,y), \tag{3a}$$

$$v(x,y,z) = -z\theta_y(x,y), \tag{3b}$$

$$w(x,y,z) = w(x,y), \tag{3c}$$

where u, v and w are the components of displacement at x, y and z directions, respectively, and θ_x and θ_y are the rotations in xz and yz planes, respectively. Since the recovered strain is considered to be within the range of the linear elastic strain, one has

$$\varepsilon_x = -z\frac{\partial \theta_x}{\partial x}, \qquad \varepsilon_y = -z\frac{\partial \theta_y}{\partial y}, \tag{4a}$$

$$\gamma_{xy} = -z\left(\frac{\partial\theta_x}{\partial y} + \frac{\partial\theta_y}{\partial x}\right), \qquad \gamma_{xz} = -\left(\theta_x + \frac{\partial w}{\partial x}\right), \qquad \gamma_{yz} = -\left(\theta_y + \frac{\partial w}{\partial y}\right). \tag{4b}$$

In addition, the following elastic stress–strain relations can be applied to both the SMA and the elastomer layers:

$$\sigma_x = \frac{E}{1-\upsilon^2}(\varepsilon_x + \upsilon\varepsilon_y), \qquad \sigma_y = \frac{E}{1-\upsilon^2}(\varepsilon_y + \upsilon\varepsilon_x), \tag{5a}$$

$$\tau_{xy} = G\gamma_{xy}, \quad \tau_{xz} = G\gamma_{xz}, \quad \tau_{yz} = G\gamma_{yz}. \tag{5b}$$

The constitutive equations for the SMA layer can be obtained by combining Eqs. (2), (4) and (5), and the constitutive equation for the elastomer layer is developed by combining Eqs. (4) and (5).

The system of equations governing the bending of the actuator can be developed by considering a differential element of the SMA/elastomer plate subject to a uniformly distributed load per unit area, q. Multiplying Eqs. (1a) and (1b) by $z\,\mathrm{d}z$, and integrating Eqs. (1a)–(1c) across each layer gives

$$\int_{h_0}^{h_1}\frac{\partial\sigma_{x1}}{\partial x}z\,\mathrm{d}z + \int_{h_0}^{h_1}\frac{\partial\sigma_{xy1}}{\partial y}z\,\mathrm{d}z + \int_{h_1}^{h_2}\frac{\partial\sigma_{x2}}{\partial x}z\,\mathrm{d}z + \int_{h_1}^{h_2}\frac{\partial\tau_{xy2}}{\partial y}z\,\mathrm{d}z - Q_x = 0, \tag{6a}$$

$$\int_{h_0}^{h_1}\frac{\partial\sigma_{y1}}{\partial y}z\,\mathrm{d}z + \int_{h_0}^{h_1}\frac{\partial\tau_{xy1}}{\partial x}z\,\mathrm{d}z + \int_{h_1}^{h_2}\frac{\partial\sigma_{y2}}{\partial y}z\,\mathrm{d}z + \int_{h_1}^{h_2}\frac{\partial\tau_{xy2}}{\partial x}z\,\mathrm{d}z - Q_y = 0, \tag{6b}$$

$$\frac{\partial Q_x}{\partial x} + \frac{\partial Q_y}{\partial y} + q = 0, \tag{6c}$$

where σ_{x1} and τ_{xy1} are the normal and shear stresses in the elastomer layer, respectively, σ_{x2} and τ_{xy2} are the normal and shear stresses in the SMA layer, respectively, Q_x and Q_y are the shear resultants and are given by

$$Q_x = \int_{h_0}^{h_1}\tau_{xz1}\,\mathrm{d}z + \int_{h_1}^{h_2}\tau_{xz2}\,\mathrm{d}z, \tag{7a}$$

$$Q_y = \int_{h_0}^{h_1}\tau_{yz1}\,\mathrm{d}z + \int_{h_1}^{h_2}\tau_{yz2}\,\mathrm{d}z. \tag{7b}$$

By combining Eqs. (2) and Eqs. (4)–(7), one obtains the following system of equations in dimensionless form for bending of the actuator:

$$A_{44}\frac{\partial}{\partial X}\left(\theta_x + \frac{\partial W}{\partial X}\right) + A_{55}\frac{\partial}{\partial Y}\left(\theta_y + \frac{\partial W}{\partial Y}\right) + \Phi = 0, \tag{8a}$$

$$\begin{aligned} &D\frac{\partial}{\partial X}\left(\frac{\partial\theta_x}{\partial X} + \upsilon_{\mathrm{e}}\frac{\partial\theta_y}{\partial Y}\right) + D_{33}\frac{\partial}{\partial Y}\left(\frac{\partial\theta_x}{\partial Y} + \upsilon_{\mathrm{n}}\frac{\partial\theta_y}{\partial X}\right) + (D_{\mathrm{A}} + D_{\mathrm{MA}}\xi)\frac{\partial}{\partial X}\left(\frac{\partial\theta_x}{\partial X} + \upsilon_{\mathrm{e}}\frac{\partial\theta_y}{\partial Y}\right) \\ &\quad + D_{\mathrm{MA}}\frac{\partial\xi}{\partial X}\left(\frac{\partial\theta_x}{\partial X} + \upsilon_{\mathrm{n}}\frac{\partial\theta_y}{\partial Y}\right) + D_{33\mathrm{MA}}\frac{\partial\xi}{\partial Y}\left(\frac{\partial\theta_x}{\partial Y} + \frac{\partial\theta_y}{\partial X}\right) + (D_{33\mathrm{A}} + D_{33\mathrm{MA}}\xi)\frac{\partial}{\partial Y}\left(\frac{\partial\theta_x}{\partial Y} + \frac{\partial\theta_y}{\partial X}\right) \\ &\quad - A_{44}\left(\theta_x + \frac{\partial W}{\partial X}\right) = 0, \end{aligned} \tag{8b}$$

Table 1
Dimensionless stiffnesses

$D = (h_0^3 - h_1^3)/(3(1-\upsilon_e^2)h_0^3)$	$D_{33} = (h_0^3 - h_1^3)/(3(1+\upsilon_e)h_0^3)$
$D_A = (h_0^3 - h_1^3)E_A/(3(1-\upsilon_e^2)h_0^3E_e)$	$D_{MA} = (h_0^3 - h_1^3)(E_M - E_A)/(3(1-\upsilon_e^2)h_0^3E_e)$
$D_{33A} = (h_1^3 - h_2^3)E_A/(3(1+\upsilon_n^2)h_0^3E_e)$	$D_{33MA} = (h_1^3 - h_2^3)(E_M - E_A)/(3(1+\upsilon_n)h_0^3E_e)$
$A_{44} = \frac{5}{4}\sum_{i=1}^{2} G_i\left[h_i - h_{i-1} - \frac{4}{3}\left(h_i^3 - h_{i-1}^3\right)\frac{1}{h^2}\right]$	$A_{55} = \frac{5}{4}\sum_{i=1}^{2} G_i\left[h_i - h_{i-1} - \frac{4}{3}\left(h_i^3 - h_{i-1}^3\right)\frac{1}{h^2}\right]$

$$D\frac{\partial}{\partial X}\left(\frac{\partial\theta_x}{\partial X}+\upsilon_e\frac{\partial\theta_y}{\partial Y}\right)+D_{33}\frac{\partial}{\partial Y}\left(\frac{\partial\theta_x}{\partial Y}+\upsilon_n\frac{\partial\theta_y}{\partial X}\right)+(D_A+D_{MA}\xi)\frac{\partial}{\partial X}\left(\frac{\partial\theta_x}{\partial X}+\upsilon_e\frac{\partial\theta_y}{\partial Y}\right)+D_{MA}\times\frac{\partial\xi}{\partial X}\left(\frac{\partial\theta_x}{\partial X}+\upsilon_n\frac{\partial\theta_y}{\partial Y}\right)+D_{33MA}\frac{\partial\xi}{\partial Y}\left(\frac{\partial\theta_x}{\partial Y}+\frac{\partial\theta_y}{\partial X}\right)+(D_{33A}+D_{33MA}\xi)\frac{\partial}{\partial Y}\left(\frac{\partial\theta_x}{\partial Y}+\frac{\partial\theta_y}{\partial Y}\right)-A_{55}\left(\theta_x+\frac{\partial W}{\partial X}\right)=0, \tag{8c}$$

where the coefficients D, D_{33}, D_A, D_{MA}, D_{33A}, D_{33MA}, A_{44}, A_{55} are defined in Table 1.

Now, consider a differential element of the SMA layer. If the heat loss on the top surface of the SMA layer is neglected, constructing the energy balance on the SMA leads to

$$C_n\frac{\partial T}{\partial t}-Q_n\frac{\partial\xi}{\partial t}-k_n\frac{\partial^2 T}{\partial x^2}-k_n\frac{\partial^2 T}{\partial y^2}+K_e(T-T_0)=P, \tag{9}$$

where

1. $C_n(\partial T/\partial t)$ is the change in the internal energy of the SMA layer. Here, $C_n = \rho_n c$, where ρ_n is the density and c is the specific heat of the SMA.
2. $-Q_n(\partial\xi/\partial t)$ is the energy contributed to the phase transformation of the SMA. Here, $Q_n = \rho_n q_n$, where ρ_n is the density and q_n is the heat of transition of the SMA.
3. $-k_n(\partial^2 T/\partial x^2) - k_n(\partial^2 T/\partial y^2)$ is the heat conduction in x and y directions through the SMA layer and k_n is the thermal conductivity of the SMA.
4. $K_e(T - T_0)$ is the quasi-steady model for heat lost by conduction through the elastomer layer. Here, $K_e = k/[t_n(h - t_n)]$, where k is the thermal conductivity of the elastomer. This model was verified in a previous publication (Wirtz et al., 1995).
5. P is the input power generated by the electric current passed through the SMA layer in the heating process. P is zero if Eq. (9) is applied to the cooling process.

Eq. (9) may be written in dimensionless form as

$$\frac{\partial\Theta}{\partial\tau}-R_{MA}\frac{\partial\xi}{\partial\tau}-\frac{\partial^2\Theta}{\partial X^2}-\frac{\partial^2\Theta}{\partial Y^2}+R_k\Theta+S-R_P=0, \tag{10}$$

where Θ is the nondimensional temperature of the SMA, τ, the dimensionless time, R_{MA}, the dimensionless heat of transition of the SMA, R_k, the dimensionless thermal conductivity of the elastomer, S, the heat sink strength which characterizes the heat conduction loss from the SMA through the elastomer to the heat sink, and R_P, the dimensionless input power to the SMA layer. The dimensionless symbols are defined in Table 2.

A linear model, providing a one-dimensional relation between the martensite fraction with temperature and stress during the phase transformation, was proposed and experimentally verified by Lin and Rogers (1991). The model for the heating and cooling transition processes is in the following forms respectively (Lin and Rogers, 1991):

Table 2
Dimensionless parameters

Quantity	M → A, heating	A → M, cooling
Time, τ	$k_n t/h^2 C_n$	$k_n t/h^2 C_n$
Temperature, Θ	$(T-M_f)/(A_f-A_s)$	$(T-M_f)/(M_s-M_f)$
Heat of transition, R_{MA}	$q_n/C_n(A_f-A_s)$	$q_n/C_n(M_s-M_f)$
Power ratio, R_P	$Ph^2/k_n(A_f-A_s)$	
Heat sink strength, S	$(M_f-T_0)/(M_s-M_f)$	$(M_f-T_0)/(M_s-M_f)$
Applied load, Φ	q/E_e	
Deflection, W	w/h	w/h
Coordinate, X	x/h	x/h
Coordinate, Y	y/h	y/h
Conductivity, R_k	$K_e h^2/K_n$	$K_e h^2/K_n$

$$\xi = 1 - \frac{T - A_s}{A_f - A_s} + \frac{\sigma}{C_A(A_f - A_s)}, \tag{11}$$

$$\xi = 1 - \frac{T - M_f}{M_s - M_f} + \frac{\sigma}{C_M(M_s - M_f)}, \tag{12}$$

where C_A and C_M are the material constants which indicate the influence of the stress on the transformation temperatures, A_s and A_f, respectively. M_s and M_f are the start and finish temperature of the phase transformation from austenite to martensite, respectively, and σ is the magnitude of stress in the SMA. Since in this study, a thin, symmetric SMA layer with symmetric loading and boundary conditions is considered, Eqs. (11) and (12) are extended to the two-dimensional case, and σ is assumed to be the hydrostatic stress. For a general case, a two-dimensional constitutive model may be employed.

By combining Eqs. (2), (4), and (5), Eqs. (11) and (12) can be rewritten in a generic form for both the heating and cooling transition processes as

$$\xi = 1 - \Theta + \frac{(h-t)}{3hC_A(A_f - A_s)(1-\upsilon_n)}[(1-\xi)E_A + E_M]\left(\frac{\partial\theta_x}{\partial X} + \frac{\partial\theta_y}{\partial Y}\right) \tag{13}$$

Eqs. (8a)–(8c), (10) and (13) form a system of equations governing the bending problem of the proposed SMA/elastomer actuator subject to both thermal and mechanical loads, where W, θ_x, θ_y, Θ and ξ are independent variables.

3. Finite element formulation

A finite element model for the system of Eqs. (8), (10) and (13) is derived by constructing the variational formulation for each of these equations. Since the system of equations is nonlinear, the coefficient matrix $[K]$ in the finite element formulation depends on the primary variables $\{W, \theta_x, \theta_y, \Theta, \xi\}$. As a result, an iterative solution procedure must be employed. In this study, an alternative procedure for solving Eqs. (8), (10) and (13) is developed. Instead of solving Eqs. (8), (10) and (13) simultaneously, Eqs. (8) and (10) are decoupled and solved separately for W, θ_x, θ_y, and Θ, by estimating an initial value for ξ at each time step. Then, Eq. (13) is used to test if the calculated W, θ_x, θ_y, Θ and the estimated ξ are the true solutions. If not, Eqs. (8) and (10) are resolved for W, θ_x, θ_y, and Θ with an improved estimation of ξ. This iteration is continued until the solution is obtained. The advantage of the proposed alternative procedure over the

conventional procedure is that the number of degrees of freedom per node of a finite element is reduced by one, and the number of iteration required for convergence is significantly less.

The variational formulation of Eqs. (8) and (10) over a typical element Ω^e is obtained by multiplying each equation by a weight function N_i ($i = 1, 2, 3, 4$) and integrating the results by parts:

$$\int_{\Omega^e} N_1\{\text{LHS of Eq. (8a)}\}\,\mathrm{d}x\,\mathrm{d}y = 0, \tag{14a}$$

$$\int_{\Omega^e} N_2\{\text{LHS of Eq. (8b)}\}\,\mathrm{d}x\,\mathrm{d}y = 0, \tag{14b}$$

$$\int_{\Omega^e} N_3\{\text{LHS of Eq. (8c)}\}\,\mathrm{d}x\,\mathrm{d}y = 0, \tag{14c}$$

$$\int_{\Omega^e} N_4\{\text{LHS of Eq. (10)}\}\,\mathrm{d}x\,\mathrm{d}y = 0. \tag{14d}$$

Substituting Eqs. (8) and (10) into Eq. (14) leads to

$$\begin{aligned}
&\int_{\Omega^e}\left\{A_{44}\frac{\partial N_1}{\partial X}\left(\theta_x+\frac{\partial W}{\partial X}\right)+A_{55}\left(\theta_y+\frac{\partial W}{\partial Y}\right)\right\}\mathrm{d}X\,\mathrm{d}Y\\
&\quad=\int_{\Omega^e} N_3\Phi\,\mathrm{d}X\,\mathrm{d}Y+\oint_{\Gamma^e} N_1\left[A_{44}\left(\theta_x+\frac{\partial W}{\partial X}\right)n_x+A_{55}\left(\theta_y+\frac{\partial W}{\partial Y}\right)n_y\right]\mathrm{d}s,
\end{aligned} \tag{15a}$$

$$\begin{aligned}
&\int_{\Omega^e}\left\{\left[(D+D_{\mathrm{A}}+D_{\mathrm{MA}}\xi)\frac{\partial N_2}{\partial X}-D_{\mathrm{MA}}\frac{\partial\xi}{\partial X}N_2\right]\frac{\partial\theta_x}{\partial X}+\left[(D\upsilon_{\mathrm{e}}+D_{\mathrm{A}}\upsilon_{\mathrm{n}}+D_{\mathrm{MA}}\upsilon_{\mathrm{n}}\xi)\frac{\partial N_2}{\partial X}\right.\right.\\
&\quad\left.-D_{\mathrm{MA}}\upsilon_{\mathrm{n}}\frac{\partial\xi}{\partial X}N_2\right]\frac{\partial\theta_y}{\partial Y}+\left[(D_{33}+D_{33\mathrm{A}}+D_{33\mathrm{MA}}\xi)\frac{\partial N_2}{\partial Y}-D_{33\mathrm{MA}}\frac{\partial\xi}{\partial Y}N_2\right]\frac{\partial\theta_x}{\partial Y}+\left[(D_{33}+D_{33\mathrm{A}}\right.\\
&\quad\left.\left.+D_{33\mathrm{MA}}\xi)\frac{\partial N_2}{\partial Y}-D_{33\mathrm{MA}}\frac{\partial\xi}{\partial Y}N_2\right]\frac{\partial\theta_y}{\partial X}+A_{44}N_2\left(\theta_x+\frac{\partial W}{\partial X}\right)\right\}\mathrm{d}X\,\mathrm{d}Y\\
&\quad=\int_{\Gamma^e} N_2\left[D\left(\frac{\partial\theta_x}{\partial X}+\upsilon_{\mathrm{e}}\frac{\partial\theta_y}{\partial Y}\right)n_x+(D_{\mathrm{A}}+D_{\mathrm{MA}}\xi)\left(\frac{\partial\theta_x}{\partial X}+\upsilon_{\mathrm{n}}\frac{\partial\theta_y}{\partial Y}\right)n_x+D_{33}\left(\frac{\partial\theta_x}{\partial Y}+\frac{\partial\theta_y}{\partial X}\right)n_y\right.\\
&\quad\left.+(D_{33}+D_{33\mathrm{MA}}\xi)\left(\frac{\partial\theta_x}{\partial X}+\frac{\partial\theta_y}{\partial X}\right)n_y\right]\mathrm{d}s,
\end{aligned} \tag{15b}$$

$$\begin{aligned}
&\int_{\Omega^e}\left\{\left[(D+D_{\mathrm{A}}+D_{\mathrm{MA}}\xi)\frac{\partial N_3}{\partial Y}-D_{\mathrm{MA}}\frac{\partial\xi}{\partial Y}N_3\right]\frac{\partial\theta_y}{\partial Y}+\left[(D\upsilon_{\mathrm{e}}+D_{\mathrm{A}}\upsilon_{\mathrm{n}}+D_{\mathrm{MA}}\upsilon_{\mathrm{n}}\xi)\frac{\partial N_3}{\partial Y}\right.\right.\\
&\quad\left.-D_{\mathrm{MA}}\upsilon_{\mathrm{n}}\frac{\partial\xi}{\partial Y}N_3\right]\frac{\partial\theta_x}{\partial X}+\left[(D_{33}+D_{33\mathrm{A}}+D_{33\mathrm{MA}}\xi)\frac{\partial N_3}{\partial X}-D_{33\mathrm{MA}}\frac{\partial\xi}{\partial X}N_3\right]\frac{\partial\theta_y}{\partial X}+\left[(D_{33}+D_{33\mathrm{A}}\right.\\
&\quad\left.\left.+D_{33\mathrm{MA}}\xi)\frac{\partial N_3}{\partial X}-D_{33\mathrm{MA}}\frac{\partial\xi}{\partial X}N_3\right]\frac{\partial\theta_x}{\partial Y}+A_{55}N_3\left(\theta_y+\frac{\partial W}{\partial Y}\right)\right\}\mathrm{d}X\,\mathrm{d}Y\\
&\quad=\int_{\Gamma^e} N_3\left[D\left(\frac{\partial\theta_y}{\partial Y}+\upsilon_{\mathrm{e}}\frac{\partial\theta_x}{\partial X}\right)n_y+(D_{\mathrm{A}}+D_{\mathrm{MA}}\xi)\left(\frac{\partial\theta_y}{\partial Y}+\upsilon_{\mathrm{n}}\frac{\partial\theta_x}{\partial X}\right)n_y+D_{33}\left(\frac{\partial\theta_x}{\partial Y}+\frac{\partial\theta_y}{\partial X}\right)n_x\right.\\
&\quad\left.+(D_{33}+D_{33\mathrm{MA}}\xi)\left(\frac{\partial\theta_x}{\partial Y}+\frac{\partial\theta_y}{\partial X}\right)n_x\right]\mathrm{d}s,
\end{aligned} \tag{15c}$$

$$\int_{\Omega^e}\left\{N_4\frac{\partial\Theta}{\partial\tau}+R_k\frac{\partial N_4}{\partial X}\frac{\partial\Theta}{\partial X}+R_k\frac{\partial N_4}{\partial Y}\frac{\partial\Theta}{\partial Y}+N_4\Theta-N_4R_{\mathrm{MA}}\frac{\partial\xi}{\partial\tau}+N_4(S-R_P)\right\}\mathrm{d}X\,\mathrm{d}Y$$
$$=\oint_{\Gamma^e}N_4R_k\left(\frac{\partial\Theta}{\partial X}n_x+\frac{\partial\Theta}{\partial Y}n_y\right)\mathrm{d}s. \tag{15d}$$

From the above variational formulations, Eq. (15), it can be seen that the specification of the expressions in the square brackets of the boundary terms constitute the natural boundary conditions, and the specifications of W, θ_x, θ_y and Θ constitute the essential boundary conditions. The terms in the natural boundary conditions can be identified with the moment, shear force resultants and heat flux:

$$\begin{aligned}
M_x &= D\left(\frac{\partial\theta_x}{\partial X}+\upsilon_{\mathrm{e}}\frac{\partial\theta_y}{\partial Y}\right)+(D_{\mathrm{A}}+D_{\mathrm{MA}}\xi)\left(\frac{\partial\theta_x}{\partial X}+\upsilon_{\mathrm{n}}\frac{\partial\theta_y}{\partial Y}\right),\\
M_y &= D\left(\frac{\partial\theta_y}{\partial Y}+\upsilon_{\mathrm{e}}\frac{\partial\theta_x}{\partial X}\right)+(D_{\mathrm{A}}+D_{\mathrm{MA}}\xi)\left(\frac{\partial\theta_y}{\partial Y}+\upsilon_{\mathrm{n}}\frac{\partial\theta_x}{\partial X}\right),\\
M_{xy} &= D_{33}\left(\frac{\partial\theta_x}{\partial Y}+\frac{\partial\theta_y}{\partial X}\right)+(D_{33}+D_{33\mathrm{MA}}\xi)\left(\frac{\partial\theta_x}{\partial Y}+\frac{\partial\theta_y}{\partial X}\right),\\
Q_x &= A_{44}\left(\theta_x+\frac{\partial W}{\partial X}\right),\qquad Q_y=A_{55}\left(\theta_y+\frac{\partial W}{\partial Y}\right),\\
q_x &= R_k\frac{\partial\Theta}{\partial X},\qquad q_y=R_k\frac{\partial\Theta}{\partial Y}.
\end{aligned} \tag{16}$$

To develop a finite element model for Eq. (15), W, θ_x, θ_y, Θ and ξ may be approximated over a two-dimensional, four-node, linear element by the following interpolation functions:

$$W=\sum_{i=1}^{4}\Phi_iW_i,\quad \theta_x=\sum_{i=1}^{4}\Phi_i\theta_{xi},\quad \theta_y=\sum_{i=1}^{4}\Phi_i\theta_{yi},\quad \Theta=\sum_{i=1}^{4}\Phi_i\Theta_i,\quad \xi=\sum_{i=1}^{4}\Phi_i\xi_i, \tag{17}$$

where Φ_i ($i=1, 2, 3, 4$) are the linear interpolation functions of the four-node element in two dimensions. Substituting Eq. (16) into Eq. (15) results in

$$\begin{bmatrix}[K^{11}] & [K^{12}] & [K^{13}]\\ [K^{21}] & [K^{22}] & [K^{23}]\\ [K^{31}] & [K^{32}] & [K^{33}]\end{bmatrix}\begin{Bmatrix}\{W\}\\ \{\theta_x\}\\ \{\theta_y\}\end{Bmatrix}=\begin{Bmatrix}\{F^1\}\\ \{F^2\}\\ \{F^3\}\end{Bmatrix}, \tag{18}$$

$$[C^1]\left\{\frac{\partial\Theta}{\partial\tau}\right\}+[C^2]\{\Theta\}+[C^3]\left\{\frac{\partial\xi}{\partial\tau}\right\}=\{F^4\}, \tag{19}$$

where

$$K_{ij}^{11}=\int_{\Omega^e}\left(A_{44}\frac{\partial\Phi_i}{\partial X}\frac{\partial\Phi_j}{\partial X}+A_{55}\frac{\partial\Phi_i}{\partial Y}\frac{\partial\Phi_j}{\partial Y}\right)\mathrm{d}X\,\mathrm{d}Y,$$

$$K_{ij}^{12}=\int_{\Omega^e}\left(A_{44}\frac{\partial\Phi_i}{\partial X}\Phi_j\right)\mathrm{d}X\,\mathrm{d}Y,$$

$$K_{ij}^{13}=\int_{\Omega^e}\left(A_{55}\frac{\partial\Phi_i}{\partial Y}\Phi_j\right)\mathrm{d}X\,\mathrm{d}Y,$$

$$K_{ij}^{21} = \int_{\Omega^e} \left(A_{44} \frac{\partial \Phi_i}{\partial X} \Phi_j \right) \mathrm{d}X\,\mathrm{d}Y,$$

$$K_{ij}^{22} = \int_{\Omega^e} \left\{ \left[\left(D + D_A + D_{MA} \sum_{k=1}^{4} \Phi_k \xi_k \right) \frac{\partial \Phi_i}{\partial X} - D_{MA} \sum_{k=1}^{4} \frac{\partial \Phi_k}{\partial X} \xi_k \Phi_i \right] \frac{\partial \Phi_j}{\partial X} \right.$$
$$\left. + \left[\left(D_{33} + D_{33A} + D_{33MA} \sum_{k=1}^{4} \Phi_k \xi_k \right) \frac{\partial \Phi_i}{\partial Y} - D_{33MA} \sum_{k=1}^{4} \frac{\partial \Phi_k}{\partial Y} \xi_k \Phi_i \right] \frac{\partial \Phi_j}{\partial Y} + A_{44} \Phi_i \Phi_j \right\} \mathrm{d}X\,\mathrm{d}Y,$$

$$K_{ij}^{23} = \int_{\Omega^e} \left\{ \left[\left(D\upsilon_e + D_A \upsilon_n + D_{MA} \upsilon_n \sum_{k=1}^{4} \Phi_k \xi_k \right) \frac{\partial \Phi_i}{\partial X} - D_{MA} \upsilon_n \sum_{k=1}^{4} \frac{\partial \Phi_k}{\partial X} \xi_k \Phi_i \right] \frac{\partial \Phi_j}{\partial Y} \right.$$
$$\left. + \left[\left(D_{33} + D_{33A} + D_{33MA} \sum_{k=1}^{4} \Phi_k \xi_k \right) \frac{\partial \Phi_i}{\partial Y} - D_{33MA} \sum_{k=1}^{4} \frac{\partial \Phi_k}{\partial Y} \xi_k \Phi_i \right] \frac{\partial \Phi_j}{\partial X} \right\} \mathrm{d}X\,\mathrm{d}Y,$$

$$K_{ij}^{31} = \int_{\Omega^e} \left(A_{55} \Phi_i \frac{\partial \Phi_j}{\partial Y} \right) \mathrm{d}X\,\mathrm{d}Y,$$

$$K_{ij}^{32} = \int_{\Omega^e} \left\{ \left[\left(D\upsilon_e + D_A \upsilon_n + D_{MA} \upsilon_n \sum_{k=1}^{4} \Phi_k \xi_k \right) \frac{\partial \Phi_i}{\partial Y} - D_{MA} \upsilon_n \sum_{k=1}^{4} \frac{\partial \Phi_k}{\partial Y} \xi_k \Phi_i \right] \frac{\partial \Phi_j}{\partial X} \right.$$
$$\left. + \left[\left(D_{33} + D_{33A} + D_{33MA} \sum_{k=1}^{4} \Phi_k \xi_k \right) \frac{\partial \Phi_i}{\partial X} - D_{33MA} \sum_{k=1}^{4} \frac{\partial \Phi_k}{\partial X} \xi_k \Phi_i \right] \frac{\partial \Phi_j}{\partial Y} \right\} \mathrm{d}X\,\mathrm{d}Y,$$

$$K_{ij}^{33} = \int_{\Omega^e} \left\{ \left[\left(D + D_A + D_{MA} \sum_{k=1}^{4} \Phi_k \xi_k \right) \frac{\partial \Phi_i}{\partial Y} - D_{MA} \sum_{k=1}^{4} \frac{\partial \Phi_k}{\partial Y} \xi_k \Phi_i \right] \frac{\partial \Phi_j}{\partial Y} \right.$$
$$\left. + \left[\left(D_{33} + D_{33A} + D_{33MA} \sum_{k=1}^{4} \Phi_k \xi_k \right) \frac{\partial \Phi_i}{\partial X} - D_{33MA} \sum_{k=1}^{4} \frac{\partial \Phi_k}{\partial X} \xi_k \Phi_i \right] \frac{\partial \Phi_j}{\partial X} + A_{55} \Phi_i \Phi_j \right\} \mathrm{d}X\,\mathrm{d}Y,$$

$$F_i^1 = \int_{\Omega^e} \Phi_i Q\,\mathrm{d}X\,\mathrm{d}Y + \oint_{\Gamma^e} \Phi_i (Q_x n_x + Q_y n_y)\,\mathrm{d}s,$$

$$F_i^2 = \oint_{\Gamma^e} \Phi_i (M_x n_x + M_{xy} n_y)\,\mathrm{d}s,$$

$$F_i^3 = \oint_{\Gamma^e} \Phi_i (M_{xy} n_x + M_y n_y)\,\mathrm{d}s, \tag{20}$$

$$C_{ij}^1 = \int_{\Omega^e} \Phi_i \Phi_j\,\mathrm{d}X\,\mathrm{d}Y,$$

$$C_{ij}^2 = \int_{\Omega^e} \left(R_k \frac{\partial \Phi_i}{\partial X} \frac{\partial \Phi_j}{\partial X} + R_k \frac{\partial \Phi_i}{\partial Y} \frac{\partial \Phi_j}{\partial Y} + \Phi_i \Phi_j \right) \mathrm{d}X\,\mathrm{d}Y,$$

$$C_{ij}^3 = -\int_{\Omega^e} R_{\mathrm{MA}} \Phi_i \Phi_j \,\mathrm{d}X\,\mathrm{d}Y,$$

$$F_i^4 = \int_{\Omega^e} R_P \Phi_i \Phi_j \,\mathrm{d}X\,\mathrm{d}Y + \oint_{\Gamma^e} R_k \Phi_i (q_x n_x + q_y n_y)\,\mathrm{d}s. \tag{21}$$

Eq. (19) is a set of time-dependent ordinary differential equations which must be further approximated to obtain a set of algebraic equations. If $\{V\}$ represents a column matrix of the undetermined parameters, the weighted average of the time derivative of $\{V\}$ at two consecutive time steps n and $n+1$ can be expressed by

$$\alpha\left\{\frac{\partial V}{\partial t}\right\}^{n+1} + (1-\alpha)\left\{\frac{\partial V}{\partial t}\right\}^{n} = \frac{\{V\}^{n+1} - \{V\}^{n}}{\Delta t_{n+1}}, \tag{22}$$

where α is assumed to be equal to 0.5. By substituting Eq. (22) into Eq. (19), one has

$$\left[K^4\right]\{\Theta\} = \left\{F^4\right\}, \tag{23}$$

where

$$K_{ij}^4 = \int_{\Omega^e} \left[\Phi_i \Phi_j + \alpha \Delta t\left(R_k \frac{\partial \Phi_i}{\partial X}\frac{\partial \Phi_j}{\partial X} + R_k \frac{\partial \Phi_i}{\partial Y}\frac{\partial \Phi_j}{\partial Y} + \Phi_i \Phi_j\right)\right] \mathrm{d}X\,\mathrm{d}Y,$$

$$F_{ij}^4 = \oint_{\Omega^e} R_P \Delta t\, \Phi_i \,\mathrm{d}X\,\mathrm{d}Y + \sum_{j=1}^{4}\left\{\int_{\Omega^e}\left[\Phi_i \Phi_j + (1-\alpha)\Delta t\left(R_k \frac{\partial \Phi_i}{\partial X}\frac{\partial \Phi_j}{\partial X} + R_k \frac{\partial \Phi_i}{\partial Y}\frac{\partial \Phi_j}{\partial Y} + \Phi_i \Phi_j\right)\right]\mathrm{d}X\,\mathrm{d}Y\right\}\Theta_j^n$$

$$+ \sum_{j}^{4}\left\{\int_{\Omega^e} R_{\mathrm{MA}} \Phi_i \Phi_j \,\mathrm{d}X\,\mathrm{d}Y\right\}\left(\xi_j^{n+1} - \xi_j^n\right). \tag{24}$$

It is observed that Eqs. (18) and (23) can be decoupled, if ξ is known. Since the solution to Eqs. (18) and (23) is a time-marching initial-value problem, a good estimation of ξ can be made based on the previous value at each time step. Therefore, Eq. (18) is solved for W, θ_x, θ_y, whereas Eq. (23) is solved for Θ. The procedure for solving Eqs. (18) and (23) in step-by-step fashion is described as follows:

1. Select an initial value for Θ^0 and ξ^0 and solve Eq. (18) for W^0, θ_x^0, θ_y^0.
2. Calculate new time $\tau_{n+1} = \tau_n + \Delta\tau$ and estimate the martensite fraction ξ_{est}^{n+1} at τ_{n+1} by the free-response model $\xi_{\mathrm{est}}^{n+1} = 1 - \Theta_{\mathrm{est}}^{n+1}$ where $\Theta_{\mathrm{est}}^{n+1}$ is obtained by solving Eq. (19) with term $\partial\xi/\partial\tau$ replaced by $-\partial\Theta/\partial\tau$.
3. Solve Eq. (18) for W^{n+1}, θ_x^{n+1}, θ_y^{n+1} and Eq. (23) for Θ^{n+1}, based on W^n, θ_x^n, θ_y^n, Θ^n and ξ_{est}^{n+1}.
4. Calculate ξ^{n+1} by Eq. (13) using W^{n+1}, θ_x^{n+1}, θ_y^{n+1}, Θ^{n+1} and ξ_{est}^{n+1}.
5. Check convergence by testing if $(\xi^{n+1} - \xi_{\mathrm{est}}^{n+1})$ is satisfied with a convergence criterion. If the convergence criterion is satisfied, repeat steps (2)–(5) with a time increment. If the convergence criterion is not satisfied, calculate the new estimated ξ_{est}^{n+1} by using the relaxation method $\xi_{\mathrm{est}}^{n+1} = \xi^{n+1} + \lambda(\xi^{n+1} - \xi_{\mathrm{est}}^{n+1})$ and repeat steps (3) and (4) until the convergence criterion is satisfied.

4. Results and discussion

To verify the finite element solution, two special cases were compared with the published closed-form solutions. Test case 1 is bending of a simply supported, isotropic plate under uniform load $q_0 = 100$ lb/in.^{2}.

The geometric dimensions of the plate are as follows: $A = 10$ in., $B = 10$ in., $h = 0.05$ in. The material properties of the plate are as follows: Young's modulus, $E = 10^6$ lb/in.^{2} and Poisson's ratio, $v = 0.3$. By setting $\xi = 1$, and the Young's modulus and Poisson's ratio of both the SMA and the elastomer layers to 10^6 lb/in.^{2}, and 0.3, respectively, Eq. (18) is solved for the dimensionless center deflection ($W^* = wEh^3/qA^4$) of the plate for three different finite element meshes of 2×2, 3×3 and 4×4 linear elements. The results listed below is the comparison between the dimensionless deflection W^* obtained by the finite element and closed-form solutions:

Finite element method			Closed-form (Timoshenko and Woinowsky-Krieger, 1959)
2×2	3×3	4×4	Classical plate theory
$W^* = 43.37$	$W^* = 43.97$	$W^* = 44.16$	$W^* = 44.34$

Test case 2 is the stress-free response of the plate for the complete heating and cooling phase transitions. With $R_P = 3$, $S = 1.5$ and $R_{MA} = 1.4$, the time response solved by the finite element formulation, Eq. (23), is the same as the closed-form solution of the stress-free response presented in a previous publication (Wirtz et al., 1993):

Heating response		Cooling response	
FEM	Closed-form	FEM	Closed-form
$\tau = 0.78$	$\tau = 0.78$	$\tau = 0.63$	$\tau = 0.63$

The thermal and mechanical responses of the SMA/elastomer actuator are obtained by solving Eqs. (18) and (23). Consider the plate consisting of the SMA layer of 55-Nitinol and the elastomer layer of Dow Corning SYLGARD. The material properties of the SMA and elastomer are listed in Table 3. The boundary conditions of the plate are assumed to be of the simply supported and thermally insulated types on all four edges.

A 4×4 mesh of linear rectangular elements is employed. Also, the Crank–Nicolson method (i.e., $\alpha = 0.5$ in Eq. (22)) is used. Although the Crank–Nicolson method is unconditionally stable, a $\Delta\tau$ is computed according to the following formula to assure a reasonable accuracy:

$$\Delta\tau \leqslant \frac{2}{\lambda_{\min}}, \tag{25}$$

where $\lambda_{\min}$ is the minimum eigenvalue of the operator $-\nabla^2$. For this study, the value of $\Delta\tau$ is selected to be 0.05.

Table 3
Thermophysical properties of 55-Nitinol and Dow Corning SYLGARD

Property	Units	55-Nitinol	SYLGARD
Density, ρ	kg/m^3	6500	1050
Specific heat, c	J/kg °C	883	1422
Thermal conductivity, k	W/m °C	17	0.146
Heat of transition, q_n	J/Kg	12 600	N/A
Material constant, C_A	MPa/°C	10.3	N/A
Material constant, C_M	MPa/°C	10.3	N/A

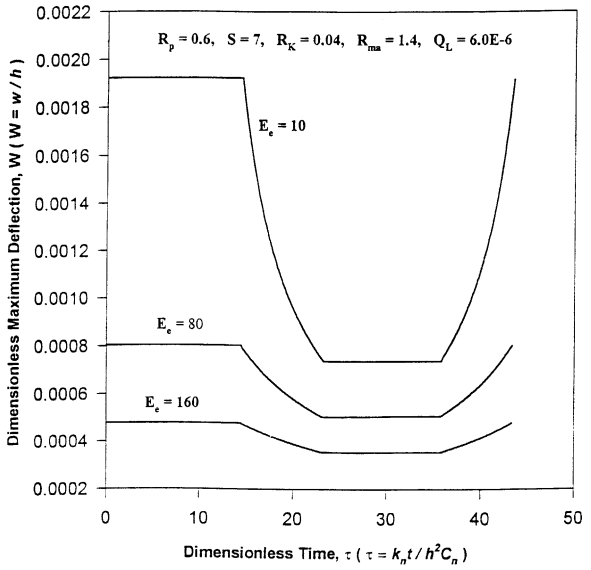

Fig. 2. The effect of the elastomer Young's modulus on the response and the maximum deflection.

The effect of elastomer layer stiffness on the center deflection of the plate for the complete heating–cooling cycle is presented in Fig. 2. The deflection remains unchanged while there is no phase transformation. The deflection increases during the phase transformation from martensite to austenite and decreases during the phase transformation from austenite to martensite. The effect on the center deflection is significant for the elastomer layer with smaller stiffnesses. The response time of a complete cycle is not significantly affected by the elastomer's stiffness.

Fig. 3 shows the dimensionless temperature and deflection responses of the actuator. The results are shown for three different dimensionless heating rates, R_P. The overall time response decreases as the heating rate increases. It can be seen that the time response changes in the heating process only, due to the heating rate increase.

Fig. 4 demonstrates the center deflection response of the actuator for three different dimensionless thermal conductivities, R_k, of the elastomer. It is shown that when the elastomer's thermal conductivity increases, the time response of the plate is decelerated during the heating response and is accelerated during the cooling process. However, the overall time response of the actuator increases, if the elastomer's thermal conductivity increases within a certain range. If the thermal conductivity exceeds a certain limit, increasing the elastomer's thermal conductivity has the opposite effect. This is demonstrated in Fig. 5.

The effect of dimensionless thermal conductivity, R_k, of the elastomer on the overall time response of the actuator is shown in Fig. 5. As it can be seen, there is a critical value for the thermal conductivity. Increasing the thermal conductivity will accelerate the overall time response of the actuator if the thermal conductivity is less than the critical value. The overall time response decelerates if the thermal conductivity exceeds the critical value. However, it is also found that the critical value is increased by increasing the heating rate.

Fig. 6 shows the effect of dimensionless thermal conductivity, R_k, of the elastomer on the overall time response of the plate for different heat sink strengths, S. It is shown that the response of the actuator is decreased and the critical value of the thermal conductivity is shifted to smaller values as the heat sink strength increases.

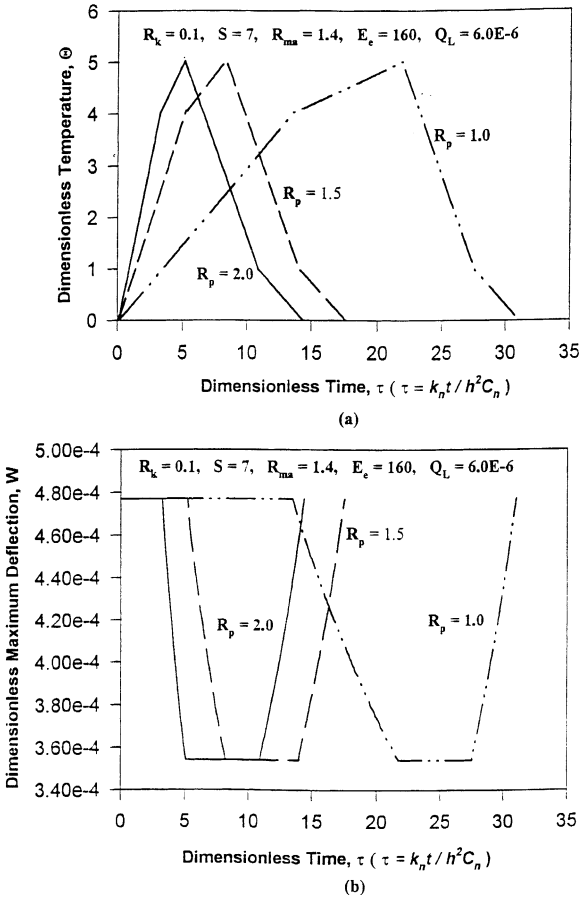

Fig. 3. The effect of the input heating on the response.

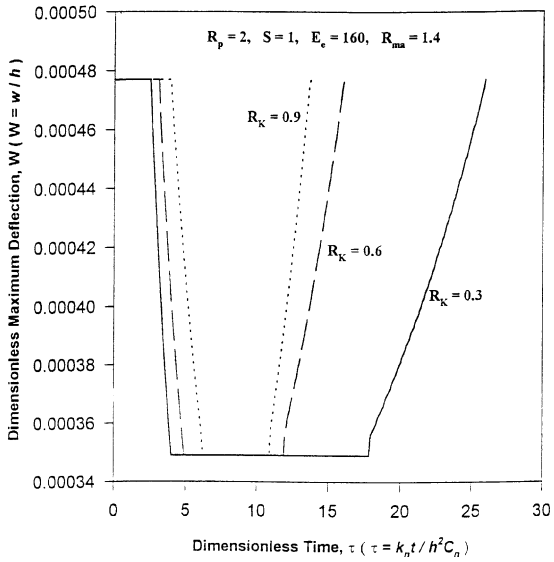

Fig. 4. The effect of the matrix thermal conductivity, k_m, on the response.

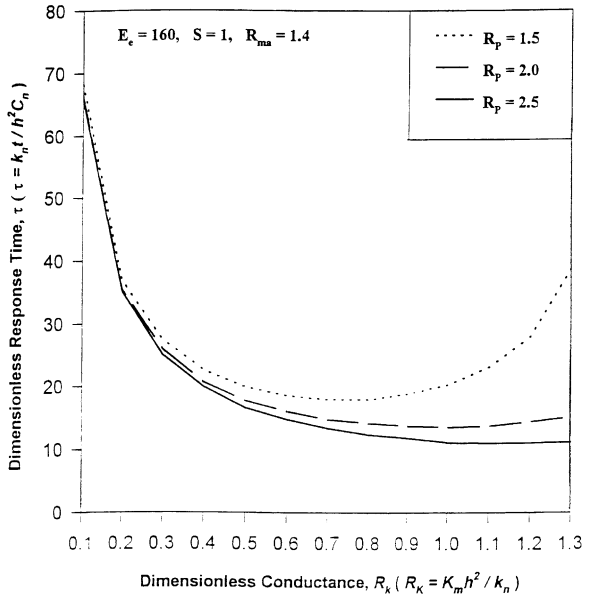

Fig. 5. The actuator response versus the elastomer conductance under different R_P.

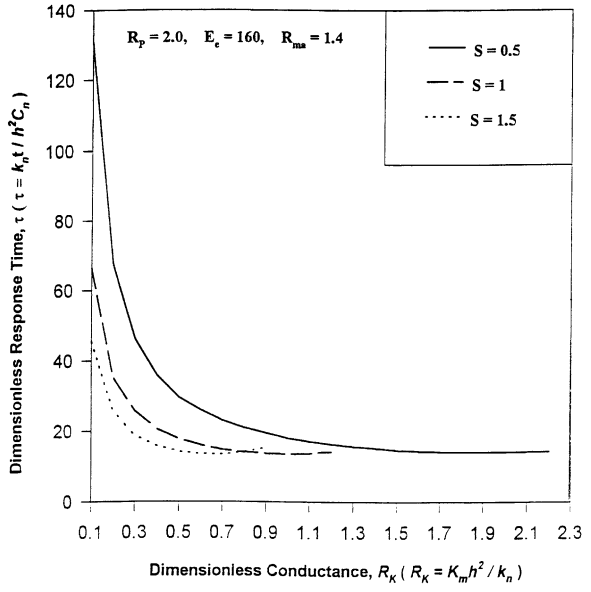

Fig. 6. The actuator response versus the elastomer conductance under different S.

Figs. 7 and 8 show the overall time response of the actuator as a function of the elastomer layer thickness ($h - t_n$) for different heat sink strengths, S, and different heating rates, R_P, respectively. The overall time response is faster if the elastomer layer thickness is smaller. Fig. 7 also shows that there is a critical value for the heat sink strength ($R = 50$), beyond which there is a minimal change on the actuator's time response.

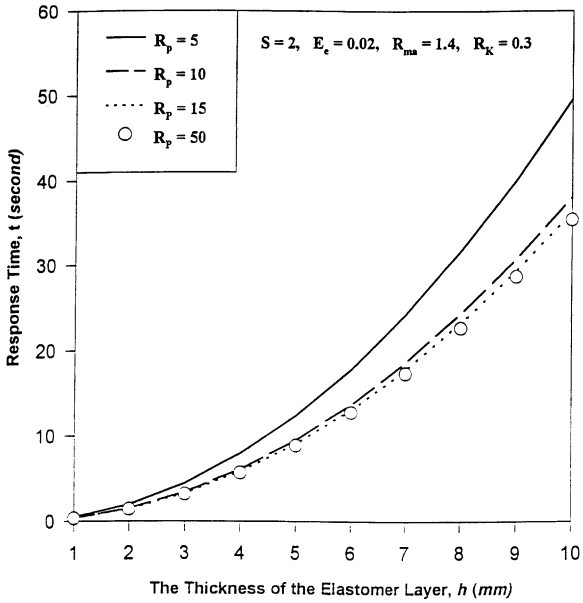

Fig. 7. The effect of the elastomer-layer thickness on the actuator response under different R_P.

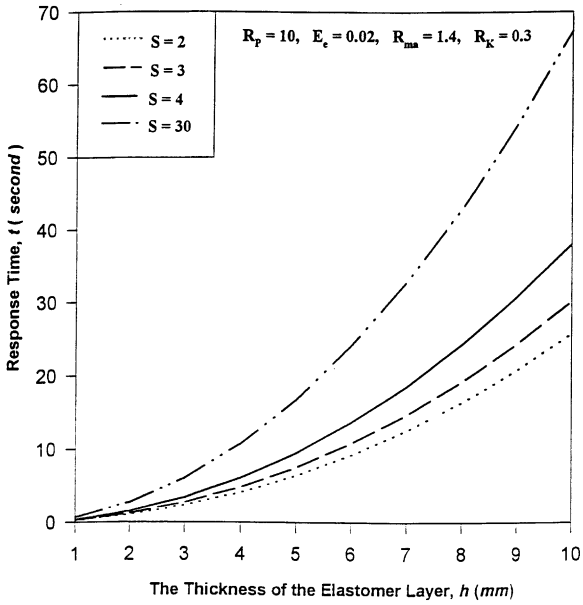

Fig. 8. The effect of the elastomer-layer thickness on the actuator response under different S.

Increasing the heat sink strength will accelerate the overall time response of the actuator more, if the heat sink strength is below the critical point, otherwise it will have the opposite effect on the overall response of the actuator. Fig. 8 shows that the response of the SMA/elastomer actuator is accelerated more by increasing the heating rate. However, the response time of the actuator is converged to a limit, if the heating

rate increases. This is because increasing the heating rate only affects the time response for the heating process.

5. Summary and conclusions

A nonlinear model for the displacement and time response of a thermally driven SMA/elastomer actuator is developed. The proposed two-dimensional actuator consists of a thin SMA layer perfectly bonded to an elastomer layer. The theoretical modeling of the actuator is based on the classical plate theory and the variable sublayer model for the two-dimensional martensitic transformation. A finite element formulation has been developed to solve the nonlinear model.

The numerical results demonstrated that the input heating, heat sink, the thermal conductivity and the thickness of the elastomer layer play important roles in controlling the time response of the SMA/elastomer actuator. In general, increasing the input heating rate accelerates the response of the actuator for the heating process, whereas increasing the heat sink strength and thermal conductivity of the elastomer accelerates the response for the cooling process. Since increasing the heat sink and the thermal conductivity of the elastomer have the inverse effect on the response of the actuator during the heating process, there is a critical point for increasing both the heat sink and the thermal conductivity of the elastomer. It is also demonstrated that increasing the heat sink and the thermal conductivity of the elastomer generally accelerates the overall response of the actuator as long as the critical point is not exceeded. It is found that decreasing the thickness of the elastomer and increasing the input power accelerate the response of the SMA/elastomer actuator.

References

Baz, A., Tampe, L., 1989. Active control of buckling of flexible beam. Proceedings of the ASME Design Technical Conference, vol. 1, DE-16. Montreal, Canada, pp. 211–218.

Ikuta, K., Shimizu, H., 1993. Two dimensional mathematical model of shape memory alloy and intelligent SMA-CAD. Proceedings of the IEEE Micro Electro Mechanical System – MEMS, Piscataway, NJ, pp. 87–92.

Lagoudas, D.C., Tadjbakhsh, I.G., 1993. Deformation of active flexible rods with embedded line actuators. Recent Developments in Stability, Vibration, and Control of Structural Systems, AMD-vol. 167. pp. 89–106.

Liang, C., Rogers, C.A., 1990. One-dimensional thermomechanical constitutive relations for shape memory materials. AIAA-90-1027-CP.

Lin, M.W., Rogers, C.A., 1991. Analysis of stress distribution in a shape memory alloy composite beam. AIAA-91-1164-CP.

Rogers, C.A., Liang, C., Jia, J., 1989. Behavior of shape memory alloy reinforced composite plates, Part 1: model formulation and control concepts. Proceeding of the 30th Structures, Structural Dynamics and Materials Conference. AIAA-89-1989.

Rogers, C.A., Baker D., 1990. Experimental studies of active strain energy turning of adaptive composites. Proceedings of the 31st Structures, Structural Dynamics and Materials Conference, Long Beach, CA, pp. 2234–2241.

Saunders, W.R., Robershaw, H.H., Rogers, C.A., 1991. Structural acoustic control of a shape memory alloy composite beam. Journal of Intelligent Materials, System and Structures 2, 508–527.

Tanaka, K., Nagaki, S., 1982. A thermomechanical description of material with internal variables in the process of phase transformation. Ingenieur Achives 51, 287–299.

Timoshenko, S., Woinowsky-Krieger, S., 1959. Theory of Plate and Shells. McGraw Hill, New York.

Wirtz, R.A., Gordaninejad, F., Wu, W., 1995. Free response of a thermally driven composite actuator. Journal of Intelligent Materials, Systems and Structures 6, pp. 398–406.

Wu, W., Gordaninejad, F., Wirtz, R.A., 1996. Modeling and analysis of a shape memory alloy–elastomer composite actuator. Journal of Intelligent Materials, Systems and Structures 7, pp. 441–447.